7

Advanced Surfactant-Modified Wet Anisotropic Etching

Bin Tang and Kazuo Sato
Nagoya University
Japan

1. Introduction

In the area of Micro Electro Mechanical Systems (MEMS), bulk micromachining and surface micromachining are two main technologies. Bulk micromachining defines structures by selectively etching inside a substrate while surface micromachining uses a succession of thin film deposition and selective etching on top of a substrate. The two technologies are quite different, resulting in different dimensions and different mechanical properties. Although bulk micromachining is usually considered to be the older technology, the two developments run parallel. This is due to the fact that the two different approaches have trade-offs. Taking an example of MEMS capacitance accelerometers, surface micromachined structures use smaller chip area, thus leaving more space for the electronics. On the other hand, in bulk micromachining the larger mass gives greater sensitivity for accelerometers and the larger area leads to larger capacitances for easy read out, which are extremely useful in the inertial device fabrication.

1.1 Wet anisotropic etching in MEMS

Bulk micromachining technology relies on isotropic or anisotropic liquid phase (wet) etching as well as by plasma phase (dry) etching in single crystalline silicon for the formation of functional shapes and patterns in many major applications. Although dry etching has penetrated the traditional territory of wet etchants, the high cost in dry etching and the difficulty in the etch rate uniformity on the whole wafer in wet isotropic etching still make wet anisotropic etching the most affordable method for the reliable production, if wet anisotropic etching can be used to deliver a similar intermediate or final structure.

The formation of crystal facets due to etching is referred to as faceting. When the primary flat of Si {100} is along the [110] direction, rectangular structures with concave corners are easily made with four (111) sidewalls and a (100) plane as the bottom. If the slow etching (111) planes meet, etching will be self-limiting to result in inverted pyramids. Etched grooves, trenches, wells and other basic structures of diaphragms (membranes), beams, and cantilevers exemplify the features of crystal plane-dependent etching. Combined with the use of mask patterns, the etch rate anisotropy becomes a most valuable property as it provides a low-cost, precise means for the production of three-dimensional shapes delimited by smooth, shiny facets, leading to complex structures with multiple functionalities, as shown in Fig. 1.

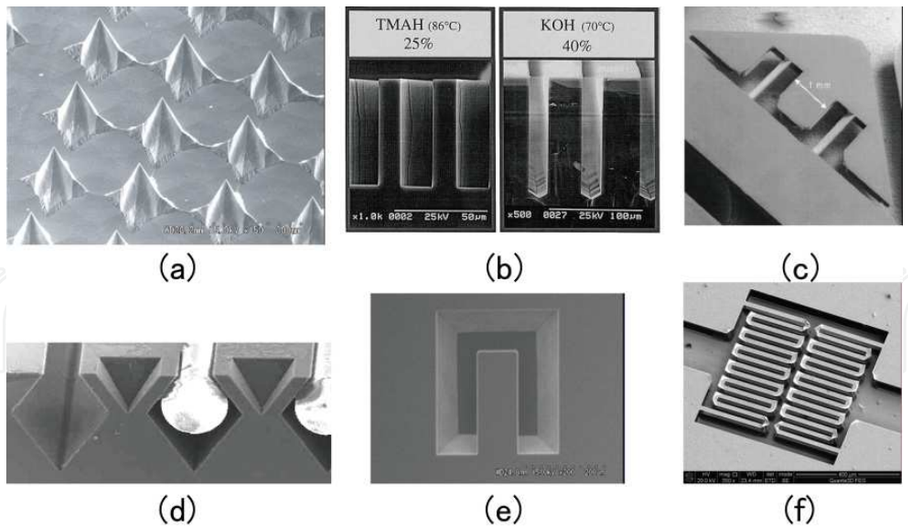

Fig. 1. Wet anisotropic etched structures for various kinds of applications: (a) microneedles for bio-medical applications, Shikida et al. 2006; (b) deep grooves, Sato et al. 1998; (c) mass-spring systems for accelerometers, Butefisch et al. 2000; (d) grooves for the optical fibre alignment, Hoffmann et al. 2002; (e) cantilever beam; (f) suspended filament beams as MEMS heaters, Lee et al. 2009.

A number of alkaline etchants have been tried for wet anisotropic etching of single crystal silicon. Some main features of wet etchants are compared in Table 1. EDP (also referred to as EPW for ethylene diamine, pyrocathecol and water) is not wildly used because of occupational safety and health hazards. Therefore, potassium hydroxide (KOH) and tetra methyl ammonium hydroxide (TMAH) are the most commonly used anisotropic etchants. Based on the ability to withstand the chemical attack by these etchants, silicon oxide (SiO_2), silicon nitride (Si_3N_4), and other metal layers (e.g. Cr, Au) have been used as masking materials. KOH is non-toxic, easy to use, provides excellent etching profiles and has a good selectivity between Si and Si_3N_4, although poor for SiO_2. In addition, KOH is incompatible with CMOS processing due to the presence of an alkali metal. Although TMAH has a lower etch rate, it has outstanding characteristics, such as a high selectivity between Si and SiO_2, and the absence of harmful ions. Hence, TMAH solutions are preferred in recent research and production.

Etchant	KOH (40 wt%)	TMAH (25 wt%)	EDP (80 wt%)
Rate (at 80 °C) μm/min	1	0.5	1 (at 115 °C)
Etching of SiO_2 mask	0	++	+
Compatibility for IC process	-	+	+
Handling (toxicity)	+	+	-
Cost	++	+	+

+:Good 0:Fair -:Poor

Table 1. Comparison of some main features of wet etchants.

1.2 Motivation of surfactant-modified etchants

With different etchants or in the conditions of different concentrations and temperatures, people could get different etching characteristics, which can be clarified as etch rate anisotropy, surface roughness and mask-corner undercut. Surface roughness improvement is important when considering the optical and tribological applications. On the other hand, the conventional design of MEMS structures fabricated by wet silicon bulk micromachining on Si {100} has sharp edge convex and concave corners. This design exhibits stress concentration at the concave corners when a load is applied, which may initiate micro cracks. By providing rounded concave corners instead of sharp ones, the stress can be reduced, thus improving the mechanical efficiency of the microstructures. In pure TMAH solutions, however, both surface roughness and mask-corner undercut are not good enough in regard to above applications. Fig. 2 illustrates anisotropic etched cantilever beam shaped patterns with mask-corners in 10 wt% TMAH at 60 °C. The etched surface is full of hillocks with an average roughness of 110nm. Therefore, many other factors have to be thought over.

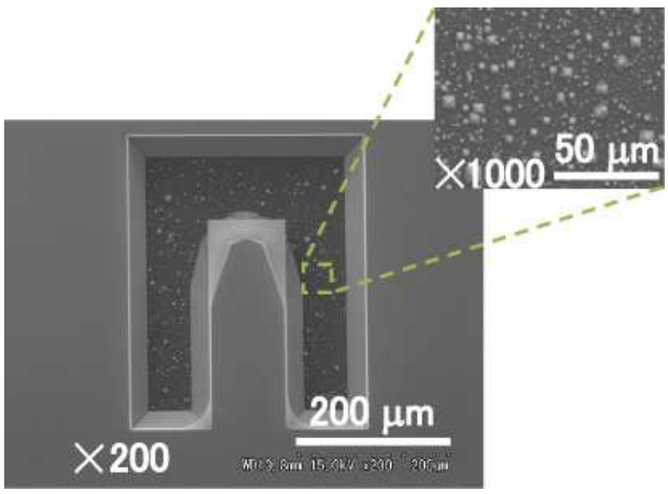

Fig. 2. Anisotropic etched cantilever beam shaped patterns with mask-corners in 10 wt% TMAH at 60 °C (etching depth = 34 μm). The upper right figure is 100 μm x 100 μm.

Among those methods for improving surface roughness and mask-corner undercut, for instance, metal impurities, alcohols, diffusion, light, pressure, microwave irradiation, corner compensation and ultrasonic irradiation et al., surfactant-modified wet anisotropic etching is more outstanding for the effects in both surface smoothness and undercut decrease, also for its stabilization of anisotropy change.

Various ionic (e.g. anionic SDSS, cationic ASPEG, etc.) and non-ionic (e.g. PEG, NC series, Triton X-100, etc.) surfactants have been investigated. Although anionic surfactants exhibit the highest etching rate, the cationic and non-ionic surfactants are suitable for TMAH solutions to improve the roughness of the etched surface owing to the excellent capacity to wet the silicon wafer. TMAH solutions with cationic and non-ionic surfactants are IC-compatible process. Furthermore, adding non-ionic surfactant to TMAH solutions can efficiently reduce undercutting at mask-corners. Such an addition is preferred when accurate profiles are required without very deep etching. Therefore, non-ionic surfactant-modified etching process attracts researchers' attention. With regard to easily handling and less toxicity, in this study, Triton X-100 is selected.

This chapter starts by providing the completely etch rate anisotropy in surfactant-modified wet etching in section 2; the mechanism behind of the change of etching characters when compared with pure etchants will be analyzed in section 3; several applications for the fabrication of new structures by using this advanced anisotropic wet etching will be presented in section 4.

2. Characterization of the etch rate anisotropy

Different etchants can give different etching properties. As one of the most important properties, the etch rate anisotropy clearly manifests the etching behavior in a concentrated solution. In this chapter, the characterization of the etch rate anisotropy is studied by using hemispherical silicon specimens, with and without surfactant in TMAH solutions. Especially, surfactant-modified etching process is analyzed in detail because of its benefit in MEMS applications.

2.1 Experimental details

The hemispherical specimen enables us to obtain the etch rate for all range of crystallographic orientations under the same etching conditions simultaneously, because all the orientations are placed on its surface. The P-type single-crystal hemispherical specimen with a diameter of 44 mm (resistivity: 6–12 Ω-cm) is used in the evaluation. The ingot of hemispheres is provided by Sumitomo Sitix Corporation. In order to produce hemispheres, it is mechanically ground, lapped and polished into mirrored surfaces with a sphericity of less than 10 μm, latitude from 0 to 90° and surface roughness of 0.005–0.007 μm in the arithmetical average by Okamoto Kogakukosakusho Corporation. The etch rate at each orientation is calculated by measuring the shape change before and after etching. The optimized etching depth should be in the range of 100–150 μm in order to avoid interference between neighboring orientations while maintaining the resolution of the geometry measurement. The shape is measured using a 3D profile machine UPMC550-CARAT (Carl Zeiss Co.) with an accuracy of less than 1.0 μm. Fig. 3 shows the locations of crystallographic orientations on the silicon hemispherical sample and a schematic view of the surface profile measurement. Area 'A' corresponds to the measurable area of the hemispherical silicon sample. The place outside the measurement zone and the bottom area are protected by a thermally grown oxide layer. The surface profile is probed every 2° of latitude ranging from 0° to 70°, and every 2° of longitude ranging from 0° to 360°. Supplements of de-ionized (DI) water into an etching bath every 2 h control the tolerance of etching temperature within 1 °C. The total numbers of probe points to be measured are 6480.

TMAH (Toyo Gosei Co. Ltd) and Triton X-100 (Amersham Biosciences) are used as the main etchant and surfactant, respectively. The Triton solution is used to prepare the surfactant-added TMAH solution. The fresh etchant is employed in every subsequent experiment.

2.2 Etch rate anisotropy

The photos of the hemispherical specimen before and after etching at 61 °C in TMAH + Triton are taken as one of the examples and presented in Fig. 4. The contour maps made by the 3D Anisotropic-Etching Simulator (FabMeister-ES) are shown in Fig. 5. Due to the crystallographic symmetry of the hemispherical specimen, only one quarter part with averaged etch rates among equivalent orientations is presented. The range of the planes

affected by surfactant adding is clearly visible. The etch rates of exact and vicinal {100} planes are almost unaffected when the surfactant is added, while the etch rates of exact and vicinal {110} planes are reduced significantly.

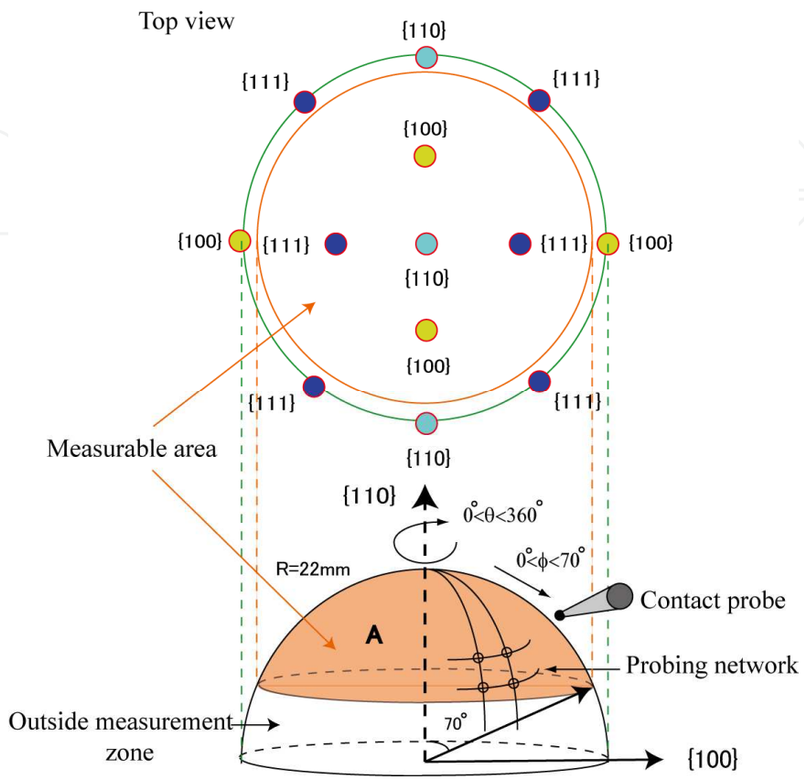

Fig. 3. Location of different crystallographic orientations on one silicon hemispherical sample and schematic view of surface profile measurement. (Reproduced with permission from IOP)

Fig. 4. Photos of the hemisphere specimen: (a) before etching and (b) after etching (etching temperature = 61 °C).

The effect of etching temperature on the etch rates is shown in Fig. 6. The etching anisotropy is influenced by temperature. The orientation of the highest etch rate is shifted toward {350} with the increase in temperature. Contrary to 71 and 81 °C, no single plane prominently appears as the highest etching rate plane at 61 °C. The etch rates of the orientations between {100} and {110} largely depend on the temperature; however, those in between {110} and {111} exhibit less dependence. It can obviously be concluded from these results that the etching anisotropy depends upon the etching temperature. This will result in different etched profiles due to the difference in etching temperatures even if the

same mask is used. Examples of measured etch rates for nine different orientations are listed in Table 2. The etch rate ratios of {mnl}/{100}, where m, n, and l are integers, increase with temperature for the planes lying between {100} and {110} (excluding {100} and {110}). On the other hand, these ratios for the planes lying between {110} and {111} are almost the same for 61 °C; however, for other temperatures (71 and 81 °C), the values vary.

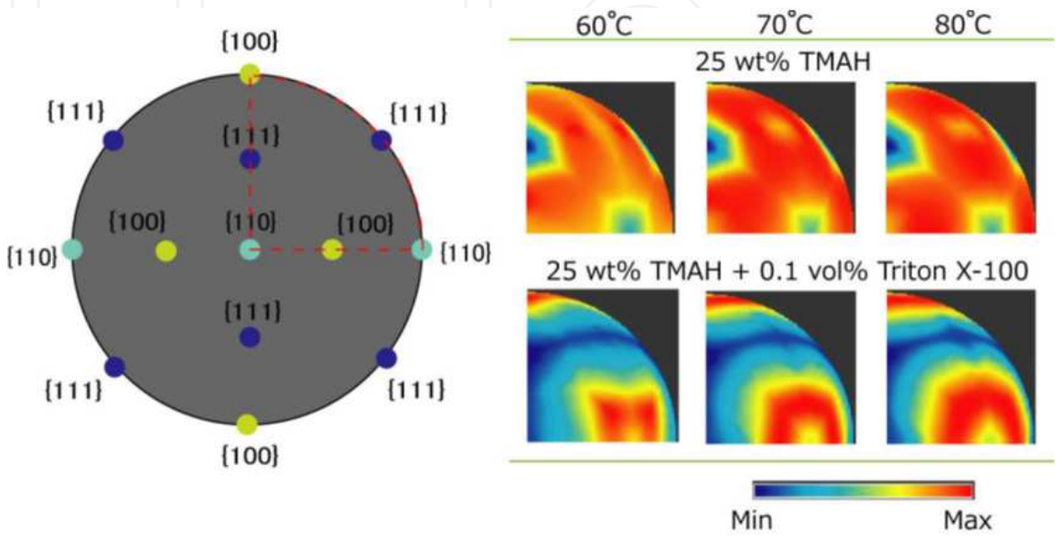

Fig. 5. Contour maps of etch rate in pure and surfactant-added TMAH solutions

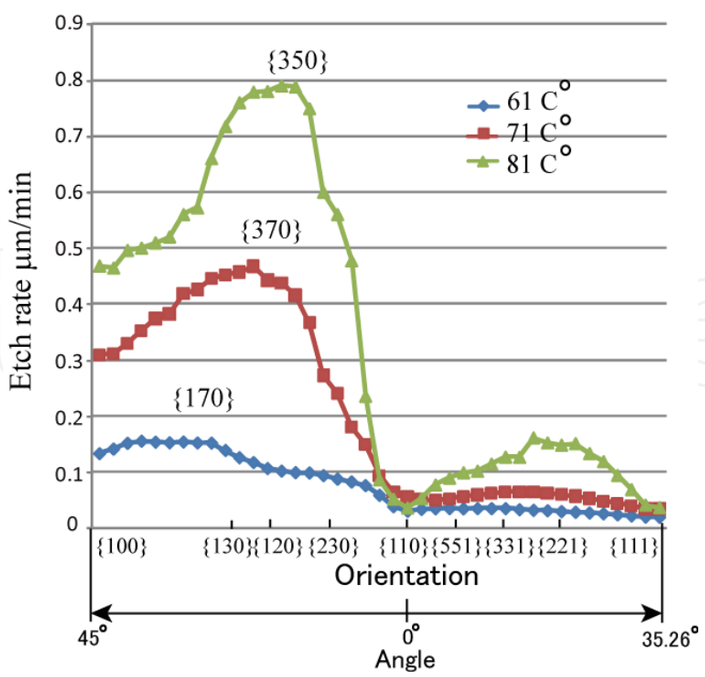

Fig. 6. Effect of temperature on the etch rate anisotropy in 25 wt % TMAH + 0.1 vol% Triton X-100.

Orientation	61°C		71°C		81°C	
	Etch rate (μm/min)	{mnl}/{100}	Etch rate (μm/min)	{mnl}/{100}	Etch rate (μm/min)	{mnl}/{100}
{100}	0.133	1.000	0.308	1.000	0.468	1.000
{130}	0.138	1.038	0.462	1.500	0.717	1.532
{120}	0.102	0.767	0.437	1.419	0.709	1.515
{230}	0.093	0.699	0.272	0.883	0.600	1.282
{110}	0.032	0.241	0.055	0.179	0.036	0.075
{551}	0.034	0.256	0.055	0.179	0.098	0.209
{331}	0.034	0.256	0.064	0.208	0.126	0.269
{221}	0.033	0.248	0.062	0.201	0.152	0.325
{111}	0.019	0.143	0.033	0.107	0.035	0.077

Table 2. Orientation- and temperature-dependent etch rates and etch rate ratios of {mnl}/{100} in TMAH + Triton solutions.

Temperature-dependent etching anisotropy is verified by fabricating 3D circular shape cavities on silicon {100} wafers. Fig. 7 shows the SEM images of circular cavities (etch depth = 100 μm) formed in Triton-added 25 wt% TMAH at 61 and 81 °C using circular shape mask opening, respectively. SEM images are taken after removal of the oxide masking layer. In the case of TMAH + Triton, the {110} and its vicinal planes emerge along <100> directions as these planes exhibit significantly low etch rates. The cavity etched at 81 °C provides better roundness than that of etched at 61 °C. This is because of improved anisotropy ({mnl}/{100}) at high temperature (Table 2). When the temperature is increased from 61 to 81 °C, the etch rate ratios of {110}/{100} and {111}/{100} are changed from 0.241 and 0.143 to 0.077 and 0.075, respectively.

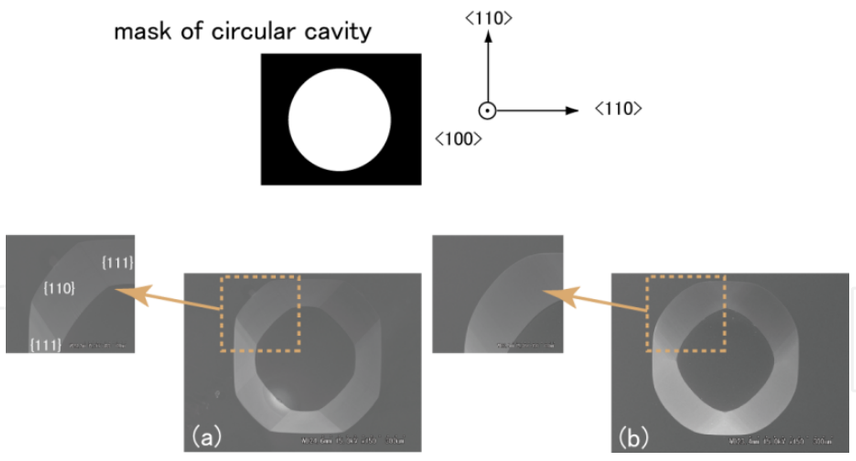

Fig. 7. Circle-like 3D microstructures in Si {100} wafers using one-step etching in 25 wt % TMAH + 0.1 vol% Triton X-100 at: (a) 61 °C and (b) 81 °C.

The Arrhenius-type dependence of etching rates for six planes {110}, {100}, {111}, {331}, {711}, and {221} is plotted in Fig. 8. The activation energy of TMAH + Triton (0.1-0.2 eV) is lower than that of pure TMAH (or KOH) solution (0.5-0.7 eV). The extreme resemblance of activation energy for {331} and {221}, which lie between {110} and {111}, may be associated with the almost same etch rates as described earlier. In particular, {110} plane has very low activation energy.

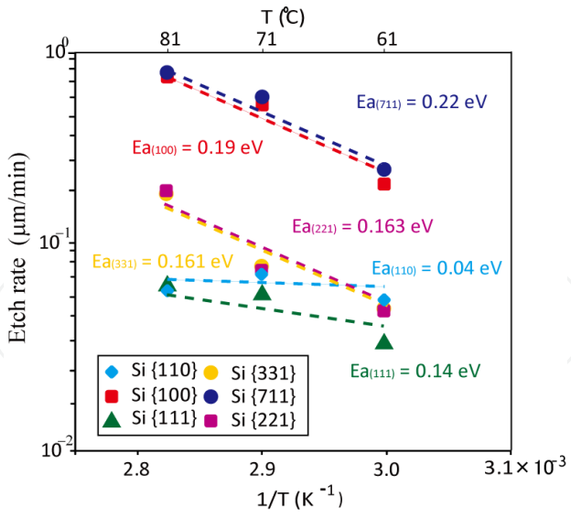

Fig. 8. The Arrhenius plot of etching rates for different planes.

3. Adsorption of surfactant molecules and its effect on etching

The change in the etching behavior of TMAH after the incorporation of the surfactant indicates that the reaction mechanism at the surface is affected by the surfactant molecules, which may block selectively some of the active surface sites, particularly those that appear on Si {110}. Triton X-100 has the following molecular structure:

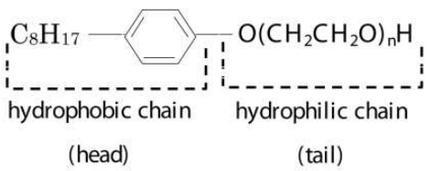

One end of the molecule is hydrophilic, and the other is hydrophobic.

3.1 Adsorption of surfactant molecules on silicon surfaces

Ellipsometry is utilized as a surface-sensitive technique in order to determine the thickness of thin films adsorbed on different surfaces at the subnanometer. Although the non-ionic surfactants do not take part in the etching reaction, their molecules are known to adsorb on the silicon surface by FT-IR observation. In this section, we report detailed ellipsometry measurements in order to determine and characterize the preferential adsorption of the non-ionic surfactant Triton X-100 on {110} and {100} surfaces before etching. The study focuses on the dependence of the thickness of the surfactant layer on various conditions such as the surfactant bath time (SBT), its temperature (T) and the use of ultrasonic agitation (UA), etc.

For experiments, we use three-inch diameter, p-type single crystalline {100} and {110} silicon wafers of 5-10 Ω-cm resistivity. These orientations are selected because of two reasons: (i) most widely used and commonly available, (ii) surfactant effects are quite different for Si {100} and Si {110}. Firstly, the wafers are diced into 13×13 mm² small samples. Thereafter, the samples are properly cleaned in chemical solutions followed by thorough rinse in de-ionized (DI) water. In this study all the containers are either glass or Teflon, depending on

the type of solution. The samples are now stored in DI water. A surfactant bath consisting of 1 vol% Triton X-100 in DI water is prepared.

The density of adsorbed surfactant molecules in the layer increases as the surfactant concentration is increased, reaching a maximum value (adsorption saturation) at a concentration that is similar in magnitude to the critical micelle concentration (CMC), typically between 0.01 vol% and 0.1 vol% (i.e. 100–1000 ppm). Increasing the surfactant concentration further results in a larger number of micelles in solution but does not affect the adsorption density at the interface. The Triton concentration value of 1 vol% in DI water is a simple choice in order to study the effect of the pre-adsorbed layer as it ensures that enough surfactant is adsorbed on the surface according to the CMC argument.

The samples are dipped in the surfactant bath at room temperature and 60 ^{o}C for different times. Prior to immersion in the Triton bath, the samples are dipped in 5% hydrofluoric (HF) acid solution for 1 min and then thoroughly rinsed in DI water. This step is attempted to make the surface hydrophobic. After the surfactant bath, the samples are gently dipped in DI water for several times to remove the most weakly adsorbed surfactant molecules from the surface. These dippings are carried out in still water in a Teflon container. The number of dippings in DI water after the surfactant bath may affect the thickness of the adsorbed layer. Therefore, the effect of the number of gentle dippings is also studied. Moreover, the effect of ultrasonic agitation during the surfactant bath is also investigated. After several dippings in DI water, the samples are dried and used for surfactant layer thickness measurements by ellipsometry. Bare silicon samples are used as reference surfaces. For the ellipsometry measurements of the obtained Triton films we used a standard geometry where the sample is placed horizontally and visible light is reflected at a grazing angle and received by the detector. The spectral analysis is performed using a commercial spectroscopic ellipsometry analyzer (MARY-102).

Although the thickness of the Triton layer (h) increases with the Surfactant Bath Time (SBT) and the thickness can be reduced by performing one or several dippings (ND), we have observed that two Triton layers of equal thickness that have been prepared in different ways, namely, (i) by only the Triton bath and, (ii) by the Triton bath followed by several dippings, have different deviations for the measured thickness in the ellipsometry measurements. When the thickness is determined by focusing the light beam on different regions of a sample without rinsing, the measurements exhibit large fluctuations (±6 Å), indicating an uneven surfactant distribution (large salience). However, the scattering range of the thickness for the samples that have been dipped is less than ±2 Å, thus indicating a more homogeneous packing of the surfactant molecules. For improved repeatability and control, we conclude already at this stage that the Triton layer should be prepared by following the second procedure (Triton bath followed by several dippings).

In order to evaluate how the thickness of the Triton layer decreases with the number of dippings, we consider a Triton layer that is initially saturated, meaning that the silicon surface has been exposed to the Triton solution for a sufficiently long time (24 h), thus ensuring that the thickness has reached its maximum value. Fig. 9(a) shows the thickness of surfactant layer as a function of the number of dippings. Here, ND = 0 means that the sample is directly dried by air. The plot shows that, for both {100} and {110} oriented wafers, a layer of finite, non-zero thickness is measured, indicating that the surfactants are adsorbed on the silicon surface. Generally, {110} samples show a thicker Triton layer, indicating a larger ability to attract surfactant molecules. Below ND = 3, the difference between Si {110} and Si {100} at the same number of dippings is small, and the thickness is high for both

orientations. For these particular measurements, the thickness changes significantly between ND = 2 and ND = 3, although it does not change much between ND = 1 and ND = 2. Above ND = 3, the thickness remains finite and constant for {110}, suggesting that the surfactant layers are strongly adsorbed –at least they cannot be easily removed by rinsing– while the thickness is vanishingly small for {100}, indicating a weaker adsorption as the surfactant layer can be easily removed. Thus, we conclude that ND = 3 is the optimal number of dippings and use it for all subsequent experiments. For ND = 3, the typical deviation in the layer thickness is roughly ±1 Å.

The surfactant layer thickness as a function of the Surfactant Bath Time (SBT) is presented in Fig. 9(b) (only ND = 3 is concerned) for two different surfactant bath temperatures (Room Temperature and 60 ^{o}C). The adsorption of the surfactant on both Si {100} and Si {110} are saturation processes, characterized by a saturation time (τ_{sat}) and a saturation thickness (h_{sat}). For non-ionic surfactants, the adsorption kinetics involve an initial fast depletion of the surfactant molecules immediately bordering the interface, followed by the diffusion of surfactant molecules from the bulk etchant to the interface and, finally, a rearrangement of the adsorbed surfactant molecules into a final packing structure. Although the actual shape of the monotonic increase of the thickness before saturation should contain valuable information about the manner how the surfactant is packed into a layer, such a study is out of the scope of the present work. From the figure, it is apparent that for the nearly same temperature {100} develops a thinner surfactant layer than {110}. The saturation thickness will become larger for smaller ND values. This observation is good in conformity with the less temperature-dependence of non-ionic surfactant adsorption.

Fig. 9(c) shows an Arrhenius plot of the saturation thickness against inverse temperature. The Arrhenius equation ($h \alpha e^{-Ea/KT}$) gives the dependence of adsorption on absolute temperature and activation energy. We find that the apparent activation energy is Ea ~ 0.15 eV for {110} while Ea ~ 0.01 eV for {100}, showing that there is clearly bigger barrier to be overcome in the adsorption process of surfactant molecules on the {110} surface. The larger activation energy for {110} suggests that chemisorption may play a role on these surfaces, whereas the small activation energy for {100} indicates that only physisorption is involved for these surfaces.

From the Arrhenius plot, it is observed that adsorption is dominantly thermal for {110}, while nearly athermal for {100}. The increase in adsorption density with temperature is mostly due to the reduction in the size of the hydration shells surrounding the surfactant molecules, especially around the hydrophilic polyethylene oxide chains. The adsorption process is a trade-off between (i) the energy reduction obtained through adsorption by increasing the number of contacts between the hydrophobic alkyl chains and the surface, and (ii) the entropy increase obtained by remaining dissolved in a more disordered state. The hydration shells are smaller at higher temperatures, resulting in less water becoming ordered per adsorbed molecule, thus allowing a larger number of adsorbed surfactant molecules at higher temperature.

Agitation is a key method that can significantly affect the wet etching quality, including the etch rate and surface morphology. The etching properties of etched surfaces with ultrasonic agitation are satisfactory and superior to no agitation. Fig. 9(d) shows the surfactant layer thickness obtained using 110 W ultrasonic cleaner (VS-D100) during residence in the surfactant bath at room temperature. After adding ultrasonic agitation, the surfactant layer thickness for {110} increases with respect to no agitation (cf. figure 3.4), indicating that appropriate forced convection can improve the adsorption of surfactant molecules.

However, for {100} the thickness is only slightly larger than without agitation, indicating little change of the surface properties. The error bars are included in figure 3.6 to stress the larger variations as compared to no agitation.
Although our study shows that a larger adsorption of Triton molecules can be obtained by using ultrasonic agitation, especially on {110}, the oscillating force results in large fluctuations in the surfactant thickness. An inhomogeneously adsorbed layer is considered a disadvantage in terms of repeatability and surface roughness control.

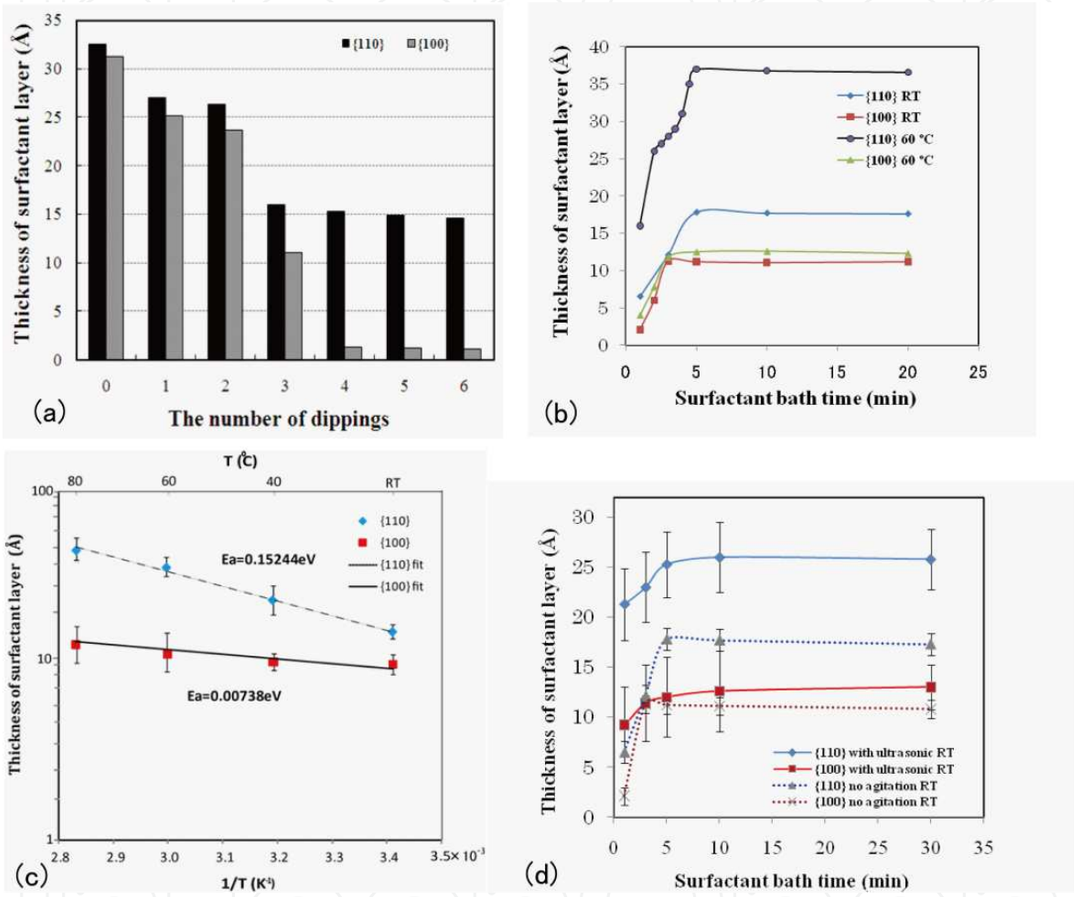

Fig. 9. Ellipsometry study: (a) thickness of the surfactant layer obtained in 1 vol% Triton as a function of the number of dipping in DI water at Room temperature; (b) surfactant layer thickness as a function of Surfactant Bath Time (SBT); (c) Arrhenius plot of the saturation thickness of surfactant; (d) comparison of the thickness of surfactant attached on the silicon surface with ultrasonic agitation at room temperature (Reproduced with permission from Elsevier).

3.2 Effect of the adsorbed surfactant layer on etching

In order to observe the effect of the adsorbed surfactant layer on the etched silicon surface morphology and etch rate, 10 wt% TMAH etchant is used at two different temperatures (room temperature and 60 °C, for both the Triton bath and the etching in TMAH) with ND = 3. The etch rates and etched surface morphology of {110} and {100} with pre-adsorbed Triton layer of different thicknesses are shown in Fig. 10 (etch depth ~ 30 ± 3 μm).

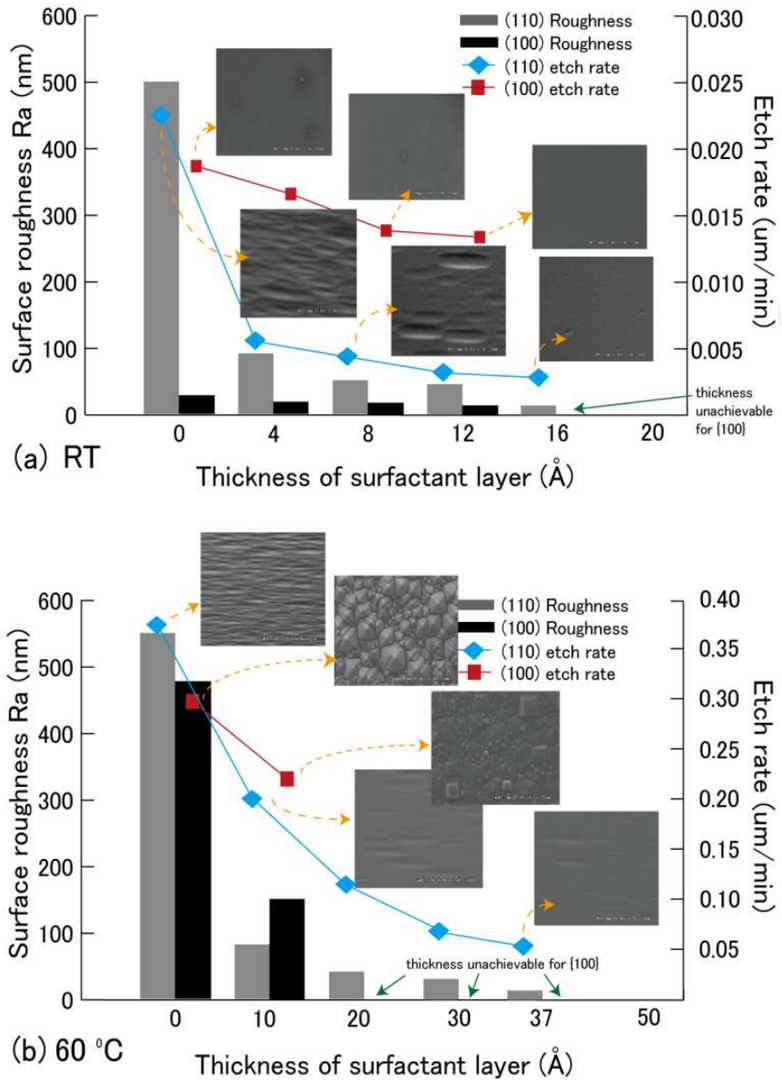

Fig. 10. Effect of pre-adsorbed surfactant layer (1 vol% Triton in DI water) on the surface roughness (Ra) and etch rate for Si {110} and Si {100} in 10 wt% TMAH: (a) room temperature; and (b) 60 °C.

For room temperature, the dramatic transformation in the surface morphology correlates directly with a strong reduction in the measured surface roughness. For {110}, it is found that typical zigzag structures emerge in pure TMAH while short pre-treatment in Triton (producing a layer thickness of 12 Å) drastically smoothens the surface, in spite of the reduced thickness of the surfactant layer. The saturated layer thickness for {110} (≈ 16 Å) produces a very smooth silicon surface (Ra ≈ 20 nm). For {100}, the surfactant pre-treatment provides some improvement in the morphology, even when the initial surface is already very smooth. Similar experiments carried out at 60 °C are shown in Fig. 10(b) (etch depth ~ 35 ± 3 μm). Although {110} shows similar surface morphologies at 60 °C and RT, the surface morphology of {100} is very different, characterized by the formation of pyramidal hillocks. Nevertheless, the roughness of both {110} and {100} is improved by the use of the surfactant layer.

In a similar manner, the thickness of the surfactant layer above the silicon surface has an effect on the etch rate in TMAH solutions after the surfactant pretreatment. For {110}, there is a significant reduction in the etch rate for thin surfactant layers. However, for {100} the reduction in the etch rate is only moderate. While {110} has a higher etch rate than {100} in pure TMAH in Fig. 10(b), the pre-treated samples show an opposite behavior, with {100} faster than {110}. This behavior is similar as for directly etching in solutions of Triton added TMAH, indicating that the dissolved surfactant is adsorbed on the surface during etching, as recently shown in FT-IR experiment. Compared with room temperature, there is a less sudden reduction in the etch rate of Si {110} wafers at 60 ^{o}C. In the case of {100}, a moderate etch rate reduction is observed at 60 ^{o}C (as for room temperature). The saturated layer thickness for {110} (≈ 37 Å) produces a very smooth silicon surface (Ra ≈ 20 nm or less).

4. Applications on MEMS

Significantly different etching behaviour of TMAH + Triton from that of traditionally used anisotropic etchants is very useful for MEMS applications in order to extend the range of 3D structures fabricated by wet etching because the surfactant is adsorbed at the silicon-etchant interface as a thin layer to act as a filter moderating the etching behaviour. In this chapter, we present three applications using surfactant-modified etchants and point out its great potential on advanced MEMS structures.

4.1 Conformal structures

The corner compensation method is the most widely used method for fabricating the sharp edge convex corners. The design and dimensions of the compensation structures require the knowledge of the undercutting ratio and its dependence on the etchant. If the design of MEMS structures does not include any rounded concave and/or sharp convex corners but a smooth etched surface is necessarily required, then the high concentration (20 – 25 wt% TMAH) should be selected for anisotropic etching. If the structures comprise rounded concave and sharp edge convex corners, the pure TMAH cannot be used due to severe undercutting.

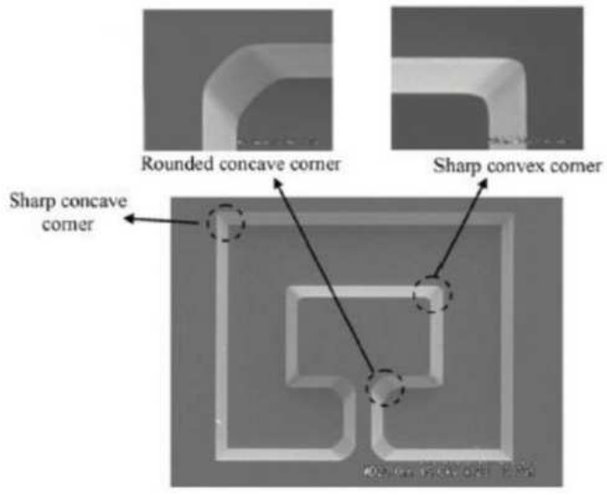

Fig. 11. Conformal mesa shape fabricated in surfactant-modified solutions.

The sharp convex corners and rounded concave corners etched in surfactant-modified TMAH solutions are shown in Fig. 11. Various kinds of etched patterns (etch depth about 35 μm) using 25 wt% TMAH without and with the surfactant are shown in Fig. 12. The undercutting at the convex corners is considerably reduced because of the changed etching anisotropy by the adsorption of surfactant molecules. This solution exhibits minimum undercutting and provides very smooth surfaces while keeping a reasonable etch rate.

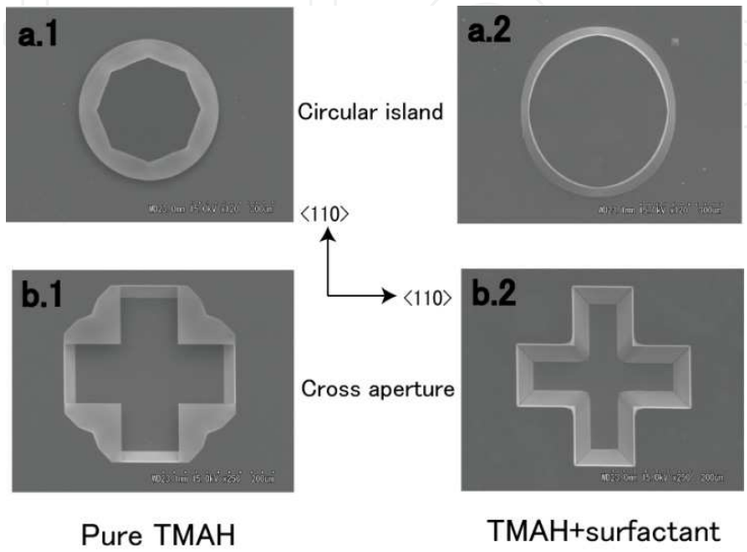

Fig. 12. Two kinds of etched patterns in pure and surfactant added 25 wt% TMAH at 60 °C (etch depth = 35 μm).

4.2 Scalloping removal for vertical micro-lens

Recently, the optical elements perpendicular to the substrate, for instance the cylindrical lens for micro-laser-scanning module applications, have been required as they can be integrated to a desired position on the same substrate using standard semiconductor processes. In order to fabricate some class of devices such as a micro-lens for optical MEMS, a highly smooth rounded column surface is required. Basically commonly used wet etchants (e.g. pure KOH and TMAH) provide very high etch rates at a rounded profile and exhibit a quite rough surface as the many faceted orientations appear on such kinds of surfaces. Hence, the removal of scalloping on rounded column surfaces is a challenging issue.

Due to the selective adsorption of surfactant molecules, the etch rate of {110} in TMAH + Triton solutions is significantly reduced. The etch rates of the planes lying between {111} and {110} at 61°C are almost same with values less than 0.05 μm. This property has been studied to remove the scalloping at the sidewalls of DRIE etched patterns on {110} silicon wafers. The study of scalloping removal is performed by short time dipping of DRIE etched patterns in TMAH + Triton. In order to investigate the effect of crystallographic directions on the surface roughness and the final shape of etched profile, a ring shape structure with internal and external diameters 200 μm and 300 μm respectively is fabricated by DRIE of about 40 μm deep. Thereafter, wet anisotropic etching is employed for 10 min in 25 wt% TMAH + 0.1 vol% Triton at 61°C. This time is long enough to clearly observe the change in profile. The SEM pictures of resultant profile and the surface morphologies of its sidewalls

at different locations are shown in Fig. 13. The qualitative analysis (SEM image) reveals that the portion between two {111} planes centered by <110> orientation (marked by F), where corrugation patterned is disappeared, is sufficiently smooth for optical applications. This is because that the planes appearing in this portion exhibit very slow and almost same etch rates for 61 ºC. Due to symmetry, the portion Q also has the smooth surface. This property is very useful for the fabrication of cylindrical lens, which can be easily integrated with other optical elements on a silicon substrate.

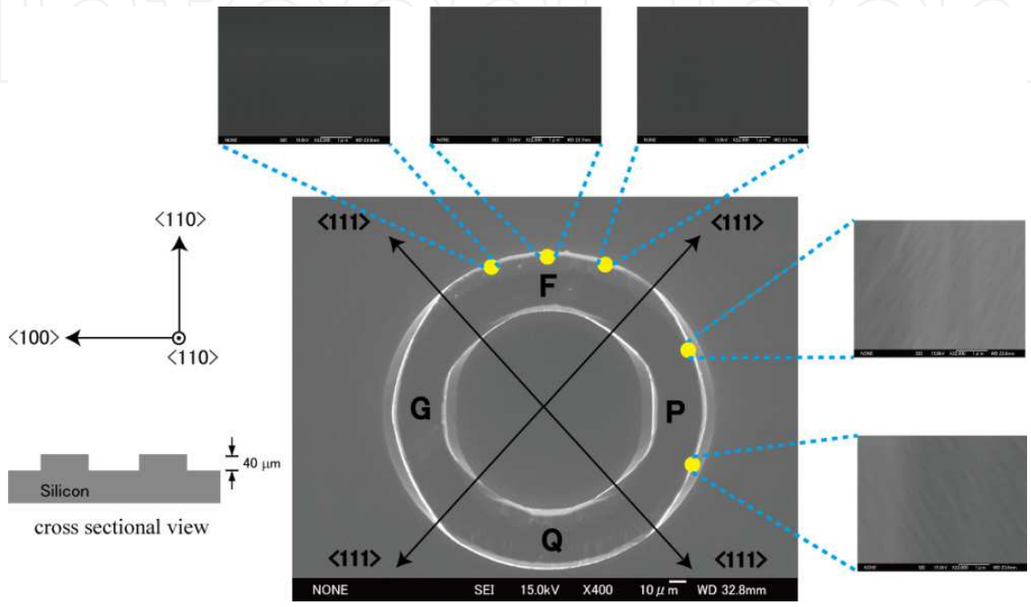

Fig. 13. SEM pictures of the ring structure and the morphologies on its different side walls after wet anisotropic etching at 61 °C.

The details of cylindrical lens portion are schematically illustrated in Fig. 14(a). The total range of the portion within two {111} planes on {110} surface is 70.54°. Since the {111} planes are the slowest etch rate planes in wet anisotropic etchants, in order to maintain the roundness of the curved profile, these planes should not be included in the design. Hence, the curved portion making an angle of 70º, is only useful portion for achieving smooth rounded vertical walls using DRIE followed by TMAH + Triton treatment. In this work, in order to demonstrate the application of surfactant-added TMAH for the removal micro-corrugation at rounded surface and the fabrication of cylindrical lens with smooth surface, the curved portion with hatched lines is selected.

The etching time for scalloping removal should be controlled accurately in order to achieve highly smooth etched surface finish while maintaining desired shape profile. In this work, the mechanism of scalloping removal is that the top area of the corrugation is etched with highest etch rate. Firstly, the left equation corresponds to the calculation of wet etching time in order to remove micro-corrugation at {110} side wall (Fig. 14(b) A-A'), where T is the etching time, $R_{\{170\}}$ is the highest etching rate at 61 °C, α is the angle between {110} and {170}, and H_1 is the height of corrugation. At 61 °C, the etching rates for {170} and {110} are the largest and smallest respectively. {170} project the corrugation, and the projected region is etched with the highest etching rate. On the other hand, {110} appears at the bottom of the

corrugation, minimizing the over-etching of the sidewall. The projected region of the corrugation is becomes small as the etching process, and it finally flattens out. In our case, α is measured as 37° and H_1 is 69.428 nm. The etching time of 42 seconds is obtained. Secondly, removing of micro-corrugation on other planes {ijk} is shown in Fig. 14(b) B-B'. Here micro-corrugation caused by DRIE is considered as the same scalloping shape. Therefore, the angle β between {ijk} and {xyz}, where {xyz} has the highest etch rate between {110} and {ijk}, is β = α = 37°. Also, the height $H_2 = H_1$ = 69.428 nm. $R_{\{ijk\}}$ is the etching rate of those planes located between {110} and {111}. Now the etching formula is described as the right equation. As noted before, etching rate of planes lying between {110} and {111} at 61 °C exhibit little variation. For this reason, we consider $R_{\{ijk\}} = R_{\{110\}}$. Another important parameter is the etch rate of highest etch rate planes in corrugated structures. Luckily, the distributions of etching rates on the {100} vicinal planes exhibit nearly identical property, which implies $R_{\{xyz\}} = R_{\{170\}}$. Thanks to the wet etching characterization in this intriguing etchants. It is feasible for the fabrication of cylindrical lens.

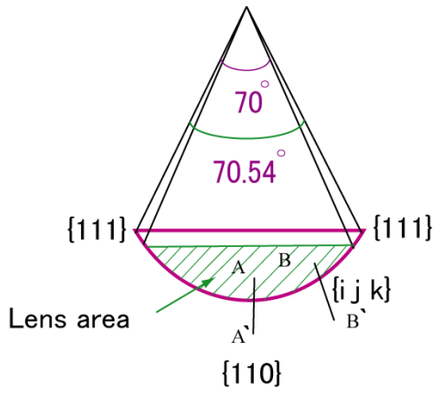

(a) Top view of cylindrical lens

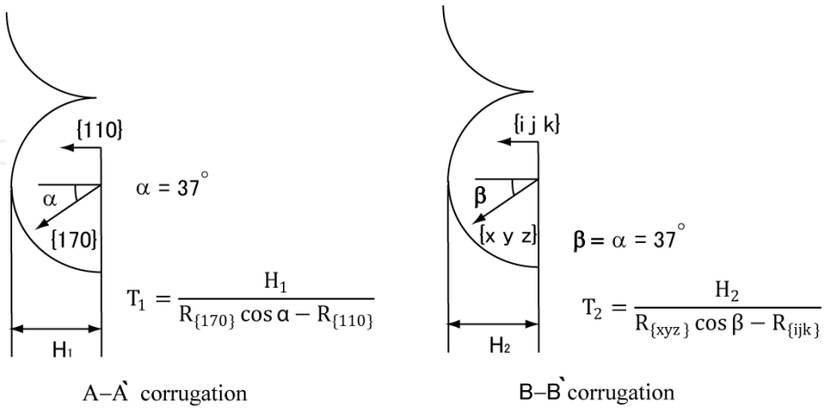

(b) Mechanism of corrugation removing

Fig. 14. (a) Schematic top view of cylindrical lens and (b) Mechanism of micro-corrugation removal by wet anisotropic etching at the sidewalls of cylindrical lens fabricated by DRIE.

Fig. 15 shows the SEM pictures and AFM measurement results of silicon surface roughness before and after wet etching. The roughness of sidewalls has been improved to about 1 nm.

This surface roughness is sufficiently enough for optical MEMS (MOEMS) applications. Thus, the small time etching in 25 wt% TMAH + 0.1 vol% Triton at 61 ºC successfully remove the micro-corrugation without altering the desired shape of the DRIE etched profile and provides almost homogeneous surface finish.

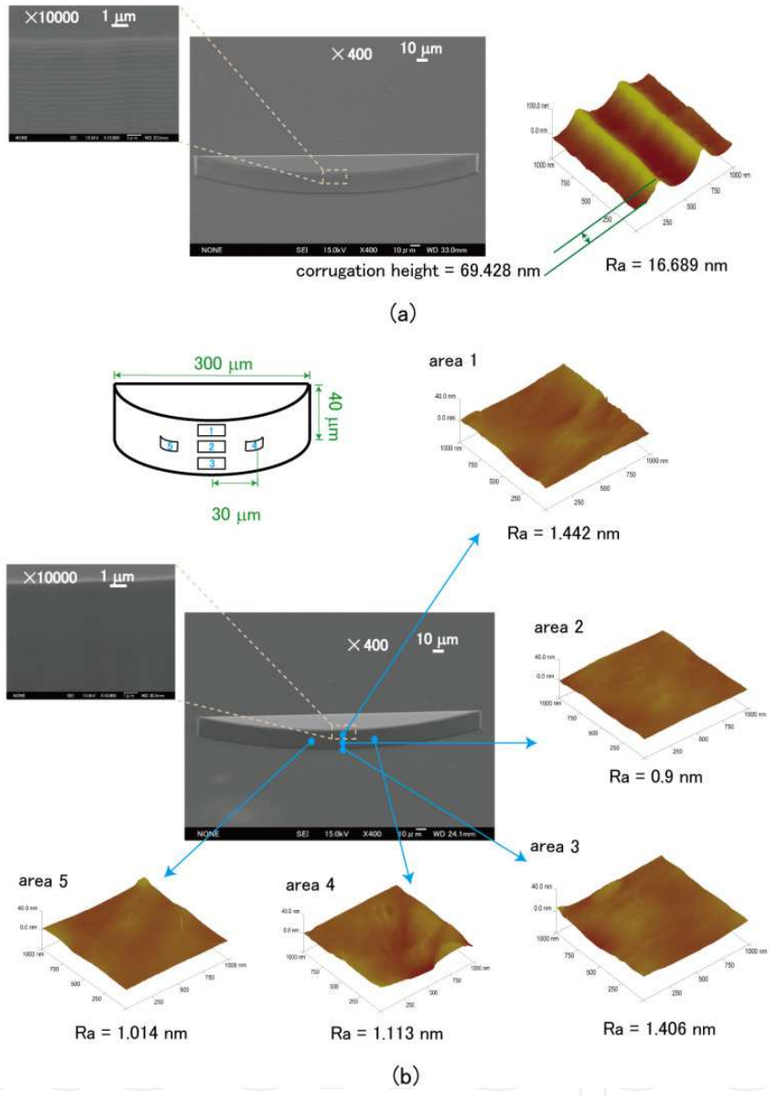

Fig. 15. SEM pictures of cylindrical lens after (a) DRIE and (b) DRIE followed by short time etching treatment in 25 wt% TMAH + 0.1 vol% Triton at 61 ºC. The AFM results reveal surface roughness at different locations of vertical sidewalls. Dimension of each zoomed figure is 9 μm x 9 μm (Reproduced with permission from IOP).

4.3 Sharp tips with high aspect ratio

(111) planes are often employed as self-stop sides in the development of MEMS structures. However, on (111) silicon wafers, if certain designated planes are exposed by dry etching, novel structures dominated by fast planes might be formed in the subsequent wet anisotropic etching. In the etchant of TMAH + Triton X-100, although (110) and its vicinal

planes are strongly affected by the adsorption of surfactant molecules, having lower etch rates than other planes, there is still a local maximum plane (221) located between (110) and (111) planes at 80°C, as shown in Fig. 16. That means (221) planes are capable of being applied to tips as the undercutting sides. The data are obtained from hemispherical samples. As we mentioned previously, there is some difference of etch rates on stressed and flat surfaces, but influence from hemispheres is limited and the relative value among the planes is sufficiently small to be ignored.

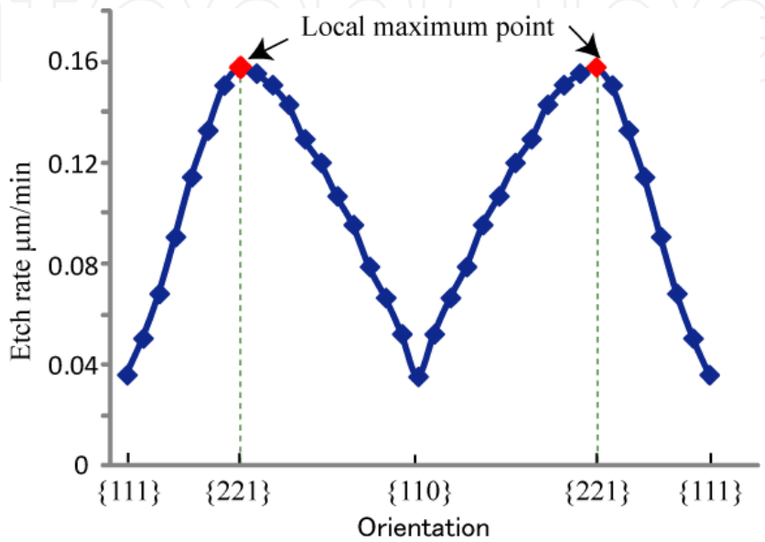

Fig. 16. Etch rate distribution between (111) and (111) in 25 wt% TMAH + 0.1 vol% Triton X-100 at 80 °C.

Here, we use a mask of equilateral triangle on (111) silicon with each side length of 60 μm in the formation of silicon tips. Wafers are firstly deep dry etched of 50 μm and then dipped into TMAH + Triton X-100 solutions. Fig. 17 shows a circularly graphic net of (111)-centered crystal orientations analyzing the wet etched shapes. Once dry etched, six fast etching (221) planes become dominant until they meet together. The angle from periphery to (221) is about 10°, leading to a much more oblique slope than conventional ones surrounded by (311) or (411) on (100) silicon wafers etched in pure KOH or TMAH. Therefore, it is allowed to fabricate silicon tips with very high aspect ratio in surfactant-modified etchants. The picture of etched sample, not over-etched, permits the examination of etched planes. The top view of one etched tip after 18 min in the TMAH + Triton X-100 at 80 °C, as shown in Fig. 18, exhibits that the etched corner is mainly composed of two planes which have fast and same etch rates. The included angle between two adjacent lines is measured as 150±2°. Note that it is on (111) silicon and the vertex angles are directed at <112>. Making the crystalline projection as a reference, this angle indicates those orientations are located at the red line. Moreover, as mentioned above, planes with the local maximum etch rates would control the control the final. Here, in the solution of TMAH + Triton, this point lies in between (111) and (110), i.e., in blue line. The junction near (221) means those planes constituting the structure which also are in the same crystal class. This result is in good persistence with previous design, indicating the truth of a new tip with very high aspect ratio.

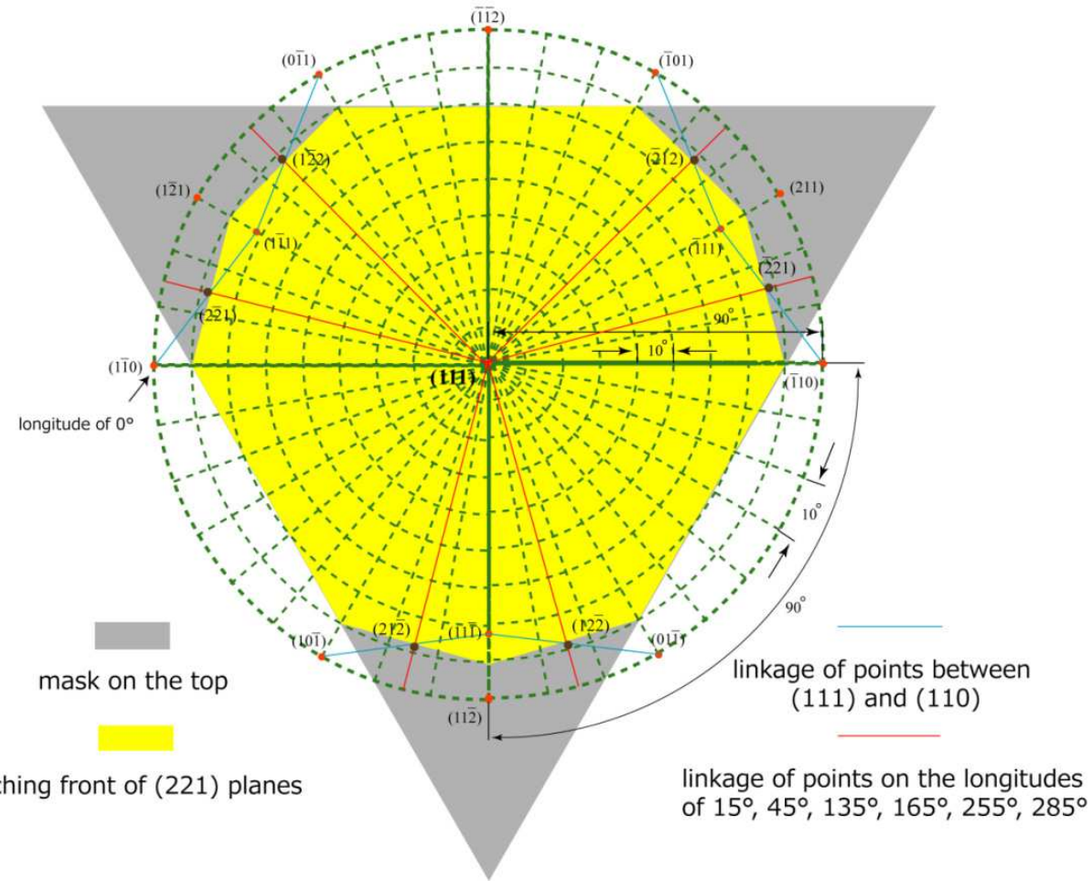

Fig. 17. A circularly graphic net of (111)-centered crystal orientations, illustrating the etched plane of (221).

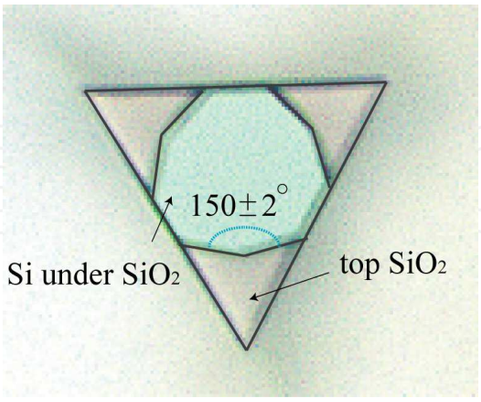

Fig. 18. One photo from optical-microscope reflecting the intermediate status during wet etching with a triangular mask on Si (111) in 25 wt% TMAH + 0.1 vol% Triton at 80 °C.

Fig. 19 shows an SEM image of the etched tip after 33 min, on which there is still a mask cap left. Furthermore, the completed tip is exhibited in Fig. 20. It is clear that the tip has a height of 30 μm, leading to the high aspect ratio of 6:1, and the front angle is measured as about

18°, which conforms with the included angle of two (221) planes. Moreover, the curvature radius of less than 10 nm is achieved without another oxidation-sharpening treatment.

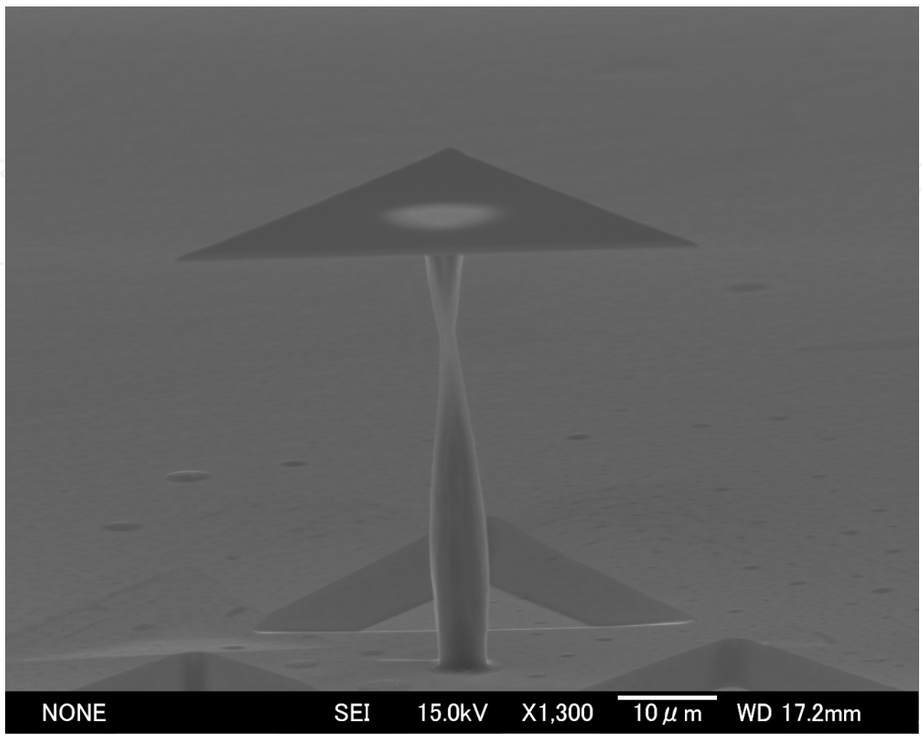

Fig. 19. An SEM image of the etched tip with a cap.

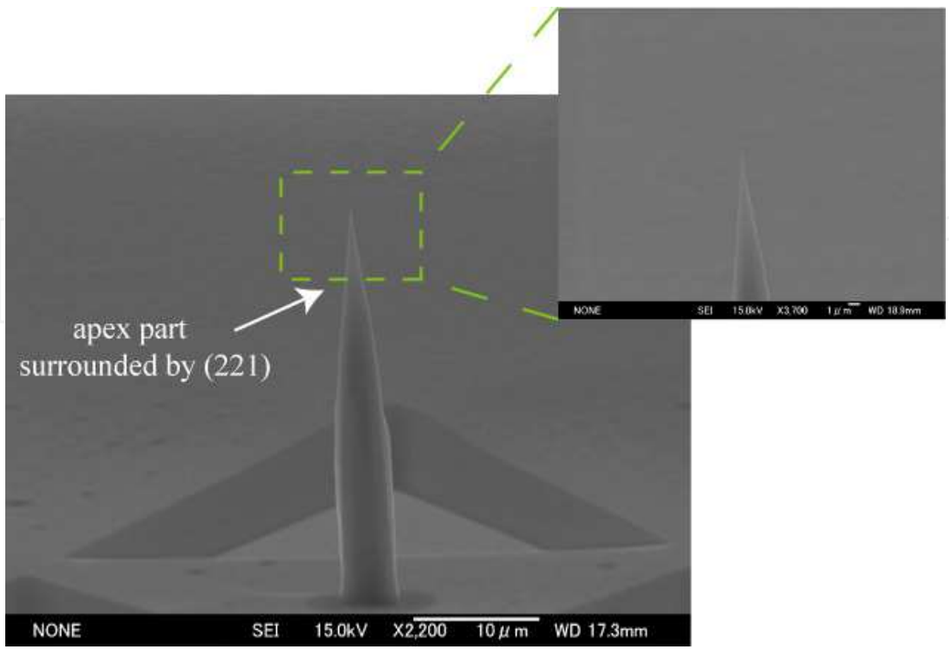

Fig. 20. A completely etched sharp tip of high aspect ratio.

5. Conclusion

In this chapter, firstly the etch rate anisotropy in surfactant-modified etch solution is investigated, showing intriguing properties that are different from that of pure alkaline solutions. The etch rates of exact and vicinal {100} planes are almost unaffected when the surfactant is added, while the etch rates of exact and vicinal {110} planes are reduced significantly. The improved anisotropy ({mnl}/{100}) at high temperature provides better conformity to the mask profile for the formation of a micro cavity. The activation energy of TMAH + Triton (0.1-0.2 eV) is lower than that of pure TMAH (or KOH) solution (0.5-0.7 eV), showing to some extent diffusion-controlled etching process.

Secondly, the underlying effect of the surfactant in etching is understood microscopically and proved macroscopically that enables manufacturing of advanced and exciting structures for MEMS. Thicknesses of surfactant layers are investigated depending on the variation of orientation, temperature et al. The pre-adsorbed surfactant layers are formed and their effects on etch rate, surface roughness and corner undercutting indicate that the dissolved surfactant is adsorbed on the surface during etching.

Finally three applications by using surfactant-modified etching process are exhibited, involving the fabrication of conformal structures, scalloping removing for vertical micro-lens, and sharp tips with high aspect ratio. Much effort will be dedicated on other potential aspects in MEMS, and more advanced devices made by this etching technique could be anticipated in future.

6. Acknowledgment

We acknowledge support by MEXT (Micro/Nano Mechatronics G-COE and grant-in-aid for scientific research (A) 19201026 and 70008053) and the Chinese High-level University Program.

7. References

Bütefisch, S.; Schoft, A. & Büttgenbach, S. Three-Axes monolithic silicon low-g accelerometer. *Journal of Microelectromechanical Systems,* Vol.9, No.4, (December 2000), pp. 551-556, ISSN 1057-7157

Gennissen, P, T, J. & French, P, J. Sacrificial oxide etching compatible with aluminium metallization, *Proceedings of IEEE 1997 9th International Conference on Solid-State Sensors and Actuators,* pp. 225–228, ISBN 0-7803-3829-4, Chicago, Illinois, USA, June 16-19, 1997

Gosalvez, M, A.; Pal, P.; Tang, B. & Sato, K. Atomistic mechanism for the macroscopic effects induced by small additions of surfactants to alkaline etching solutions. *Sensors and Actuators A*, Vol.157, No.1, (January 2010), pp. 91-95, ISSN 0924-4247

Gosalvez, M, A.; Tang, B.; Pal, P.; Sato, K.; Kimura Y. & Ishibashi, K. Orientation and concentration dependent surfactant adsorption on silicon in aqueous alkaline solutions: explaining the changes in the etch rate, roughness and undercutting for MEMS applications. *Journal of Micromechanics and Microengineering,* Vol.19, No.12, (December 2009), pp. 125011, ISSN 1361-6439

Hoffmann, M. & Voges, E. Bulk silicon micromachining for MEMS in optical communication systems. *Journal of Micromechanics and Microengineering,* Vol.12, No.4, (July 2002), pp. 349-360, ISSN 1361-6439

Inagaki, N. ; Sasaki, H. ; Shikida, M. & Sato, K. Selective removal of micro-corrugation by anisotropic wet etching, *Proceedings of IEEE 2009 15th International Conference on Solid-State Sensors, Actuators and Microsystems,* pp. 751-754, ISBN 978-1-4244-4193-8, Denver, Colorado, USA, June 21-25, 2009

Lee, K, N.; Lee, D, S.; Jung, S, W.; Jang, Y, H.; Kim Y, K. & Seong, W, K. A high-temperature MEMS heater using suspended silicon structures. *Journal of Micromechanics and Microengineering,* Vol.19, No.11, (November 2009), pp. 115011, ISSN 1361-6439

Ohara, J. ; Kano, K. & Takeuchi, Y. Development of fabrication process for integrated micro-optical elements on Si substrate. *Sensors and Actuators A*, Vol.143, No.1, (May 2008), pp. 77-83, ISSN 0924-4247

Pal, P. & Sato, K. Various shapes of silicon freestanding microfluidic channels and microstructures in one step lithography. *Journal of Micromechanics and Microengineering,* Vol.19, No.5, (May 2009), pp. 055003, ISSN 1361-6439

Pal, P.; Sato, K.; Gosalvez, M, A.; Kimura, Y.; Ishibashi, K.; Niwano, M.; Hida, H.; Tang, B. & Itoh, S. Surfactant adsorption on single crystal silicon surfaces in TMAH solution: Orientation-dependent adsorption detected by in-situ infra-red spectroscopy, *Journal of Microelectromechanical Systems,* Vol.18, No.6, (December 2009), pp. 1345-1356, ISSN 1057-7157

Pal, P.; Sato, K.; Gosalvez, M, A.; Tang, B. & Hida, H. Advanced MEMS applications using orientation dependent adsorption of surfactant molecules in TMAH solution, *Proceedings of 2010 5th Asia-Pacific Conference on Transducers and Micro-Nano Technology*, Perth, Australia, July 6-9, 2010

Park, J.; Park, K.; Choi, B.; Koo, K.; Paik, S.; Park, S.; Kim, J. & Dan Cho, D. A novel fabrication process for ultra-sharp, high-aspect ratio nano tips using (111) single crystalline silicon, *Proceedings of IEEE 2003 12th International Conference on Solid-State Sensors, Actuators and Microsystems,* pp. 1144-1145, ISBN 0-7803-7731-1, Boston, Massachusetts, USA, June 8-12, 2003

Petersen, K, E. Silicon as a mechanical material. *Proceedings of IEEE,* Vol.70, No.5, (May 1982), pp. 420–457, ISSN 0018-9219

Resnik, D.; Vrtacnik, D.; Aljancic, U.; Mozek, M. & Amon, S. The role of Triton surfactant in anisotropic etching of {110} reflective planes on (1 0 0) silicon. *Journal of Micromechanics and Microengineering,* Vol.15, No.6, (June 2005), pp. 1174-1183, ISSN 1361-6439

Sarro, P, M.; Brida, D.; Vlist, W, V, D. & Brida, S. Effect of surfactant on surface quality of silicon microstructures etched in saturated TMAHW solutions. *Sensors and Actuators A*, Vol.85, No.1-3, (August 2000), pp. 340-345, ISSN 0924-4247

Sato, K.; Shikida, M.; Yamashiro, T.; Asaumi, K.; Iriye, Y. & Yamamoto, M. Anisotropic etching rates of single-crystal silicon for TMAH water solution as a function of crystallographic orientation. *Sensors and Actuators A,* Vol.73, No.1-2, (October 1998), pp. 131-137, ISSN 0924-4247

Sato, K.; Uchikawa, D. & Shikida, M. Change in orientation–dependent etching properties of single–crystal silicon caused by a surfactant added to TMAH solution. *Sensors and Materials*, Vol.13, No.5, (May 2001) pp. 285–291, ISSN 0914- 4935

Seidel, H.; Csepregi, L.; Heuberger, A. & Baumgartel, H. Anisotropic etching of crystalline silicon in alkaline solutions: I. Orientation dependence and behavior of passivation layers. *Journal of The Electrochemical Society,* Vol.137, No.11, (November 1990), pp. 3612–3626, ISSN 1945-7111

Shikida, M. ; Sato, K. ; Tokoro, K. & Uchikawa, D. Difference in anisotropic etching properties of KOH and TMAH solutions. *Sensors and Actuators A*, Vol.80, No.2, (March 2000), pp. 179–188, ISSN 0924-4247

Shikida, M.; Hasada, T. & Sato, K. Fabrication of a hollow needle structure by dicing, wet etching and metal deposition. *Journal of Micromechanics and Microengineering,* Vol.16, No.10, (October 2006), pp. 2230-2239, ISSN 1361-6439

Tabata, O.; Asahi, R.; Funabashi, H.; Shimaoka, K. & Sugiyama, S. Anisotroplc etching of silicon in TMAH solutions. *Sensors and Actuators A,* Vol.34, No.1, (July 1992), pp. 51-57, ISSN 0924-4247

Tanaka, H.; Abe, Y.; Inoue, K.; Shikida, M. & Sato, K. Effects of ppb–level metal impurities in aqueous potassium hydroxide solution on the etching of Si{110} and {100}. *Sensors and Materials*, Vol.15, No.1, (January 2003) pp. 43–51, ISSN 0914- 4935

Tang, B.; Amakawa, H.; Shikida, M.; Hida, H; Inagaki, N.; Pal, P. & Sato, K. Characterization of etching anisotropy in a surfactant-added TMAH solution, and its application to scalloping reduction, *Proceedings of 2010 5th Asia-Pacific Conference on Transducers and Micro-Nano Technology*, Perth, Australia, July 6-9, 2010

Tang, B.; Gosalvez, M, A.; Pal, P.; Itoh, S.; Hida, H.; Shikida, M. & Sato, K. Adsorbed surfactant thickness on a Si wafer dominating etching properties of TMAH solution, *Proceedings of IEEE 2009 20th International Symposium on Micro-Nano Mechatronics and Human Science*, pp. 48-52, ISBN 978-1-4244-5094-7, Nagoya, Japan, Nov 9-11, 2009

Tang, B.; Pal, P.; Gosalvez, M, A.; Shikida, M.; Sato, K.; Amakawa, H. & Itoh, S. Ellipsometry study of the adsorbed surfactant thickness on Si{110} and Si{100} and the effect of pre-adsorbed surfactant layer on etching characteristics in TMAH. *Sensors and Actuators A*, Vol.156, No.2, (December 2009), pp. 334-341, ISSN 0924-4247

Tang, B.; Sato, K.; Tanaka H. & Gosalvez, M, A. Fabrication of sharp tips with high aspect ratio by surfactant-modified wet etching for the AFM probe, *Proceedings of IEEE 2011 24th International Conference on Micro Electro Mechanical Systems,* pp. 328-331, ISBN 978-1-4244-9632-7, Cancun, Mexico, January 23-27, 2011

Tang, B.; Shikida, M.; Sato, K.; Pal, P.; Amakawa, H.; Hida, H. & Fukuzawa, K. Study of surfactant-added TMAH for applications in DRIE and wet etching-based micromachining. *Journal of Micromechanics and Microengineering,* Vol.20, No.6, (June 2010), pp. 065008, ISSN 1361-6439

Yang, C, R.; Chen, P, Y.; Yang, C, H.; Chiou, Y, C. & Lee, R, T. Effects of various ion–typed surfactants on silicon anisotropic etching properties in KOH and TMAH solutions. *Sensors and Actuators A*, Vol.119, No.1, (March 2005), pp. 271-281, ISSN 0924-4247

Yang, C, R.; Yang, C, H. & Chen, P, Y. Study on anisotropic silicon etching characteristics in various surfactant-added tetramethyl ammonium hydroxide water solutions. *Journal of Micromechanics and Microengineering,* Vol.15, No.11, (November 2005), pp. 2028-2037, ISSN 1361-6439

Zubel, I. & Kramkowska, M. The effect of isopropyl alcohol on etching rate and roughness of (100) Si surface etched in KOH and TMAH solutions. *Sensors and Actuators A*, Vol.93, No.2, (September 2001), pp. 138-147, ISSN 0924-4247

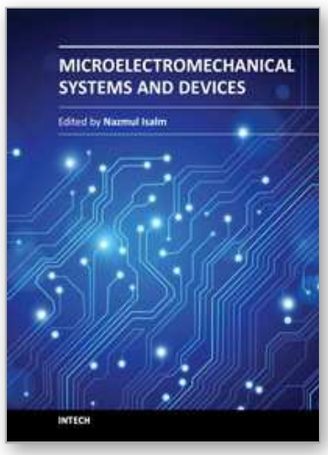

Microelectromechanical Systems and Devices

Edited by Dr Nazmul Islam

ISBN 978-953-51-0306-6
Hard cover, 480 pages
Publisher InTech
Published online 28, March, 2012
Published in print edition March, 2012

The advances of microelectromechanical systems (MEMS) and devices have been instrumental in the demonstration of new devices and applications, and even in the creation of new fields of research and development: bioMEMS, actuators, microfluidic devices, RF and optical MEMS. Experience indicates a need for MEMS book covering these materials as well as the most important process steps in bulk micro-machining and modeling. We are very pleased to present this book that contains 18 chapters, written by the experts in the field of MEMS. These chapters are groups into four broad sections of BioMEMS Devices, MEMS characterization and micromachining, RF and Optical MEMS, and MEMS based Actuators. The book starts with the emerging field of bioMEMS, including MEMS coil for retinal prostheses, DNA extraction by micro/bio-fluidics devices and acoustic biosensors. MEMS characterization, micromachining, macromodels, RF and Optical MEMS switches are discussed in next sections. The book concludes with the emphasis on MEMS based actuators.

INTECH
open science | open minds

InTech Europe
University Campus STeP Ri
Slavka Krautzeka 83/A
51000 Rijeka, Croatia
Phone: +385 (51) 770 447
Fax: +385 (51) 686 166
www.intechopen.com

InTech China
Unit 405, Office Block, Hotel Equatorial Shanghai
No.65, Yan An Road (West), Shanghai, 200040, China
中国上海市延安西路65号上海国际贵都大饭店办公楼405单元
Phone: +86-21-62489820
Fax: +86-21-62489821

IntechOpen